

Out-of-plane conductivity in single-crystal $\text{YBa}_2\text{Cu}_3\text{O}_7$

S. J. Hagen, T. W. Jing, Z. Z. Wang, J. Horvath, and N. P. Ong
Department of Physics, Princeton University, Princeton, New Jersey 08544
 (Received 9 November 1987; revised manuscript received 22 January 1988)

The resistivity anisotropy has been measured in seven single crystals of $\text{YBa}_2\text{Cu}_3\text{O}_7$. We find that the anisotropy is between 56 and 110 at 290 K, increasing to ~ 250 just above T_c (90–93 K). While the out-of-plane resistivity ρ_c is close to the Mott limit, the large in-plane resistivity ρ_{ab} (120–150 $\mu\Omega\text{cm}$ at 290 K) implies a large metallic parameter ($k_F l \sim 31$) and long electronic mean free path (67 Å at 100 K). Both ρ_c and ρ_{ab} are well described by the equation $\rho = A/T + BT$ recently proposed by Anderson and Zou.

The electronic properties of the oxides $\text{La}_{2-x}\text{Sr}_x\text{CuO}_4$ and $\text{YBa}_2\text{Cu}_3\text{O}_7$ are currently of great interest because of the high superconducting transition temperatures (T_c) observed in these unusual compounds.^{1,2} In recent months,^{3,4} several studies on single crystals of $\text{YBa}_2\text{Cu}_3\text{O}_7$ have appeared. Tozer *et al.*,⁴ in particular, have reported the temperature dependence of the out-of-plane resistivity ρ_c and the in-plane resistivity ρ_{ab} . In this paper we report more extensive measurements on single-crystal $\text{YBa}_2\text{Cu}_3\text{O}_7$ emphasizing the values of the anisotropy and the behavior of ρ_c vs T in several samples. We derive values for the metallic parameter $k_F l$ as well as the mean free path l .

The measurements were performed on single crystals grown by a flux method⁵ based on BaO. By dissolving presynthesized $\text{YBa}_2\text{Cu}_3\text{O}_7$ powder (10 to 15% of total weight) in the molten flux at a temperature below 1000°C, and slowly cooling at a rate of 10°C/h the supersaturated solution in an oxygen flow we obtain well-formed crystals of both $\text{YBa}_2\text{Cu}_3\text{O}_7$ and BaCuO_{2+y} together with lesser amounts of CuO crystals. The composition of the three types of crystals was established by electron microprobe analysis in a scanning electron microscope energy dispersive spectrometer (SEMEDS). The $\text{YBa}_2\text{Cu}_3\text{O}_7$ crystals grow as rectangular prisms of average size ($a \times b \times c$) $500 \times 500 \times 80 \mu\text{m}^3$ (Fig. 1). The larger crystals of size $1600 \times 1600 \times 100 \mu\text{m}^3$ are readily removed by tapping the bottom of the inverted crucible. Back-reflected x-ray Laue diffraction⁶ reveals that the c axis is aligned normal to the large crystal face, with extensive twinning about the 110 axis within the a - b plane as previously reported.⁷ Close examination of the Laue diffraction patterns failed to reveal Bragg spots associated with regions of the sample in which the c axis lies parallel to the large face. We conclude that such misaligned domains are insignificant in our samples.

In contrast with previous reports we find that all our as-grown crystals measured directly after pulling from the crucible have a transition term T_c between 90 and 93 K with transition widths (90% to 10%) between 0.2 and 0.5 K. A separate run to "oxygen anneal" the samples in an effort to raise T_c is unnecessary. (It may, in fact, degrade a high-quality sample as shown by a recent far-infrared reflectivity study.⁸ Annealing in an oxygen flow occurs, of course, during the original cool-down of the crucible.)

The degree of orthorhombicity can be estimated from the angle $\theta [= \pi/2 - 2 \arctan(a_2/a_1)]$ between a and b in adjacent twinned domains.⁷ (a_1 , a_2 , and a_3 are the unit-cell dimensions along a , b , and c .) The Laue pattern of our as-grown crystals shows strong twinning with $\theta = 2^\circ$ consistent with a sizable orthorhombicity $(a_1 - a_2)/a_1 = 3.4\%$. Besides the sharp transition in individual crystals we also found excellent reproducibility from sample to sample in T_c and the values of ρ_{ab} and ρ_c . Typical room-temperature values of ρ_{ab} (100–150 $\mu\Omega\text{cm}$) are significantly lower than previously reported either for single crystals or sintered samples. Some crystals were measured after two months and found to display little shift in T_c (less than 0.2 K).

Contacts with resistances $\sim 5 \Omega$ were made by soldering gold wires (25 μm diameter) directly to the crystal surface with pure In. Rather than grouping all contacts on a single face normal to a or b , we attached two contact pads (diameter 30–100 μm) on each of the two faces normal to c to minimize the distortion effect of finite contact size along c (Fig. 2, inset). To eliminate errors due to thermal emf we used the conventional phase-sensitive ac technique (with currents 200–420 μA and frequency 19–25 Hz). We verified that the resistance was Ohmic up to our highest current. After stabilization at each temperature, the resistance with the current nominally parallel



FIG. 1. Scanning electron micrograph of a typical crystal grown by the flux method. The as-grown crystals are superconducting above 90 K and orthorhombic with $\theta \sim 2^\circ$ (see text).

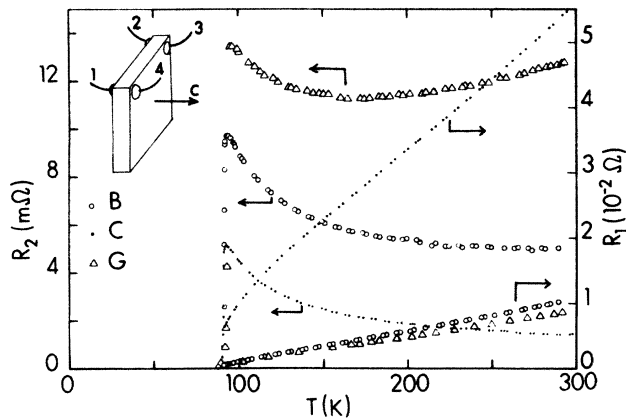


FIG. 2. The observed resistances R_1 and R_2 vs temperature in three single crystals of $\text{YBa}_2\text{Cu}_3\text{O}_7$. The inset shows the contact geometry. The dimensions of the top face are a and c . To measure R_1 (R_2), the current leads are 1 and 2 (2 and 3). The sharp increase in R_2 as T decreases is controlled by the ratio $x = (c/a)(\rho_c/\rho_{ab})^{1/2}$ (see text).

and normal to the a - b plane (R_1 and R_2 , respectively) was measured. ρ_{ab} and ρ_c were then computed from R_2/R_1 using Montgomery's technique.^{9,10}

Figure 2 shows the raw data for the resistances R_1 and R_2 in 3 samples. In all seven samples, both R_1 and R_2 fall sharply to zero at T_c . The fractional increase in R_2 as T decreases to 90 K (and the ratio R_2/R_1 at 290 K) varies substantially from sample to sample because of differences in the ratio a/c . When Montgomery's equations are used to transform (R_1, R_2) to (ρ_{ab}, ρ_c) both the ρ_{ab} - T and ρ_c - T profiles are quite similar in all the samples (Fig. 3). The relevant parameters and sample dimensions are reported in Table I. In all samples, ρ_c goes through a shallow minimum at 150 K, increasing slightly as T approaches T_c . The room-temperature value of ρ_{ab} is 100–150 $\mu\Omega$ cm (vs 450 in Ref. 4) while the anisotropy ρ_c/ρ_{ab} at 290 K is between 56 and 110 (vs 30). The slope of ρ_{ab} vs T is 0.4–0.6 $\mu\Omega$ cm/K. The anisotropy (which

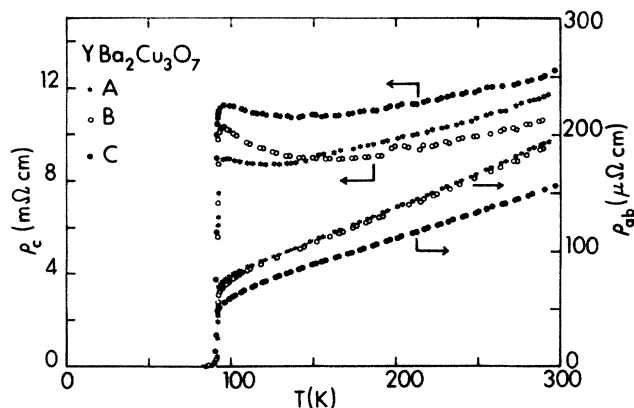


FIG. 3. The resistivities ρ_{ab} and ρ_c computed from R_1 and R_2 using Montgomery's equations. The anisotropy at 290 K is given in the table.

increases to a value between 200 and 250 at T_c in our samples) is more comparable with those commonly encountered in quasi-one-dimensional systems [10^3 in $\text{K}_0.3\text{MoO}_3$ (Ref. 11); 10^4 in $(\text{TMTSF})_2\text{ClO}_4$ at 1 K (Ref. 12)] than with the two-dimensional systems such as the dichalcogenides. However, the difference in sign between $d\rho_{ab}/dT$ and $d\rho_c/dT$ in $\text{YBa}_2\text{Cu}_3\text{O}_7$ is most unusual. It is not encountered, for instance, in the one-dimensional systems.

Because measurement of the conductivity components is difficult in highly anisotropic crystals, we discuss the possible sources of errors relevant to the crystal habit here. In the Montgomery technique the anisotropic solid is mapped onto an equivalent isotropic solid whose equipotential surfaces are computed by considering an infinite array of image charges. It is instructive to examine the solutions of Logan, Rice, and Wick¹⁰ in the two limits $x > 1$ and $x < 1$ [where x , defined as the ratio of the sides of the equivalent isotropic solid, equals $(c/a)(\rho_c/\rho_{ab})^{1/2}$]. When $x > 1$, the ratio R_2/R_1 exceeds 1 (thick sample limit). To leading order in the nome $q = e^{-\pi x}$, we have

$$R_1 = [16(\rho_{ab}\rho_c)^{1/2}/(\pi b)] \exp(-\pi x), \quad (1)$$

$$R_2 = \rho_c(c/ab) - [4(\rho_{ab}\rho_c)^{1/2} \ln 2]/(\pi b). \quad (2)$$

The term $\rho_c(c/ab)$ in Eq. (2) is the expected result when $c \gg ab$ while the second term is a correction. Thus, the R_2 - T profile is only slightly distorted from the corresponding ρ_c - T profile in this limit. In contrast, R_1 is exponentially suppressed as the anisotropy ρ_c/ρ_{ab} increases (T decreases). This is the case of sample G here and in Ref. 4. (The exponential suppression of R_1 is especially evident in the data of Ref. 4 which show R_1 becoming too small to measure below 150 K with a 500 μA current.) When $x < 1$ (thin sample limit) we perform the exchanges ($a \leftrightarrow c$), ($R_1 \leftrightarrow R_2$), ($\rho_{ab} \leftrightarrow \rho_c$) everywhere in Eqs. (1) and (2). Now R_2 is exponentially enhanced by the factor $e^{-\pi/x}$ as the anisotropy increases while R_1 is equal to ρ_{ab} (a/bc) minus the last term in Eq. (2). This behavior is quite evident in samples B and C here (see Fig. 2). Quite generally, when R_1 and R_2 differ substantially, the temperature dependence of the higher observed resistance is little distorted from that of the resistivity along that direction. However, in the other direction, the observed resistance is an exponential function of the anisotropy (either $e^{-\pi x}$ or $e^{-\pi/x}$), and therefore greatly distorted from the corresponding resistivity. Thus, in systems in which the anisotropy is large and T dependent, the observed resistance in one direction is always exponentially enhanced or suppressed. This exponential factor is a potential source of error in calculating ρ_c and ρ_{ab} if the leads are misaligned or the current paths are strongly distorted by large inhomogeneities within the sample. We studied 7 samples with aspect ratios a/c varying from 8 to 16 to check the reliability and reproducibility of our results. The nome $q = e^{-\pi x}$ may be taken as a measure of the distortion factor to be expected. With $\rho_c/\rho_{ab} \sim 100$, q varies from 0.14 (when $a/c = 16$) to 0.02 ($a/c = 8$). Errors, if present, should lead to an order-of-magnitude or greater variation in the calculated ρ_c and ρ_{ab} among the seven samples. Instead, in all samples the magnitudes of ρ_c (or

TABLE I. Sample dimensions and parameters obtained from fits to Eqs. (3) for single crystals of $\text{YBa}_2\text{Cu}_3\text{O}_7$. T_c for all samples lie between 91 and 93 K.

Sample	$a \times b \times c$ (μm^3)	A_{ab} ($\Omega \text{ cm K}$)	A_c	B_{ab} ($\Omega \text{ cm/K}$)	B_c	ρ_c/ρ_{ab} ($T=290 \text{ K}$)
A	460×450×50	1.87×10^{-3}	0.58	6.38×10^{-7}	3.40×10^{-5}	60
B	630×640×75	1.99×10^{-3}	0.73	6.24×10^{-7}	2.76×10^{-5}	56
C	390×400×25	1.73×10^{-3}	0.78	5.09×10^{-7}	3.66×10^{-5}	82
D	640×550×60	2.62×10^{-3}	0.73	6.46×10^{-7}	2.91×10^{-5}	56
E	590×410×40	2.54×10^{-3}	1.01	4.71×10^{-7}	3.22×10^{-5}	100
F	700×370×50	2.00×10^{-3}	0.64	4.18×10^{-7}	2.13×10^{-5}	110
G	690×600×75	2.01×10^{-3}	1.08	8.14×10^{-7}	6.74×10^{-5}	95

ρ_{ab}) are within 30% of each other at any T (with the exception of G). The anisotropy at room temperature also showed good reproducibility (56 to 110). Since it is unlikely that random inhomogeneities or contact misalignment errors could lead to the same “erroneous” ρ_c vs T profiles in all seven samples with such different aspect ratios we believe that these results confirm the intrinsic nature of the ρ_c vs T behavior and the anisotropy values.

The remarkable difference between the temperature dependence of ρ_{ab} and ρ_c is rarely encountered, even among the highly anisotropic systems which have been studied in the last decade. For example, in $\text{K}_{0.3}\text{MoO}_3$ (Ref. 11) and $(\text{TMTSF})_2\text{ClO}_4$ (Ref. 12) the resistivity (in weak electric fields) parallel and perpendicular to the chain axes have temperature coefficients of the same sign at all T (either both metallic or both semiconducting). In the dichalcogenides the same is true (with the possible exception of 4H-TaS_2). Within a simple Bloch-Boltzmann approach our values for both the anisotropy and ρ_{ab} provide a determination of the in-plane mean free path l of the charge carriers. At 100 K, ρ_{ab} equals $50 \mu\Omega \text{ cm}$. The very large anisotropy indicates that the energy dispersion along c is negligible. From the relation $(h/e^2)/(2\rho_{ab}/a_3) = k_F l$, appropriate for two-dimensional systems (where e^2/h is the natural unit for conductance and k_F the Fermi wave vector), we find $k_F l = 31$ at 100 K. Further, assuming one carrier per unit cell, we have $k_F = 4.6 \times 10^7 \text{ cm}^{-1}$ which implies that $l = 67 \text{ \AA}$. Contrary to earlier pictures of these oxides as “barely metallic” systems with very short l (derived from the low conductivity measured in sintered samples) we find that the large metallic parameter $k_F l$ places $\text{YBa}_2\text{Cu}_3\text{O}_7$ deep in the metallic side of the Ioffe-Regel limit, at least for the in-plane transport. However, σ_c [$100 (\Omega \text{ cm})^{-1}$] is comparable to the Mott minimum conductivity $\sigma_{\min} \sim 0.3e^2/(ha_3) = 97 (\Omega \text{ cm})^{-1}$. Thus, at the simplest level, the anisotropy points to coherent band transport in the $\text{Cu}-\text{O}$ plane and a nonmetallic transport mechanism normal to the planes.

The large value of $k_F l$ notwithstanding, we draw the conclusion that our results are inconsistent with band-theory calculations. Allen, Pickett, and Krakauer¹³ calculated from the band structure a significant anisotropy (5.6–15), but nowhere as large as reported here (120 to 250 near T_c). More significantly, the anomalous T dependence of ρ_c is problematical. As long as the interplane overlap integral is nonzero one should expect metallic be-

havior for transport along c , despite the large effective mass. This is inconsistent with the observed decrease in σ_c with decreasing T . It does not appear possible in the Block-Boltzmann approach to obtain simultaneously a nonactivated conduction mechanism between planes that decreases with T , and a metallic conduction mechanism within the plane. The temperature dependence of σ_c also rules out conventional interplane tunneling of carriers (which is T independent). The charge carrying excitations are strongly confined to the CuO plane; the mechanism for the confinement is of course a central issue. The variation of ρ_c with T implies that this mechanism is T sensitive, becoming increasingly effective at low T . (We note that there is no evidence from Laue diffraction for strong disorder along c . Absence of strong lattice disorder is also indicated by the large values of l and $k_F l$ derived from ρ_{ab} . Thus conventional localization effects along c are rather unlikely.)

A particularly interesting mechanism for out-of-plane transport has been suggested by Anderson and Zou.¹⁴ In the resonating-valence-bond theory¹⁵ for the normal state the charge carriers are hole bosons which are confined to each CuO plane. For transport between planes, Anderson and Zou propose that the tunneling of physical electrons is required. This proceeds by the merging of a hole boson

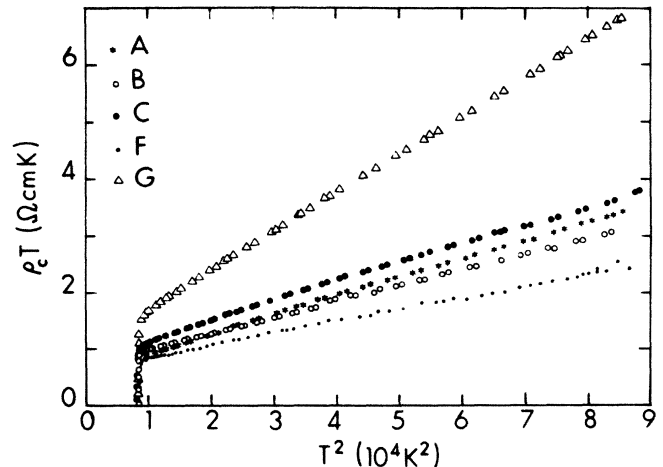


FIG. 4. The out-of-plane resistivity ρ_c plotted as $\rho_c T$ vs T^2 to test Eq. (3) in five single crystals of $\text{YBa}_2\text{Cu}_3\text{O}_7$.

(spin zero, charge 1) with a spin excitation ("spinon" with spin $\frac{1}{2}$, charge 0) to form a physical electron which then tunnels to an adjacent plane. The T dependence of σ_c arises from the spinon density which is linear in T . In practice a measurement of the resistivity along one of the axes unavoidably picks up a component from the other axes. Anderson and Zou have suggested the following fits to the observed resistivity ρ_{ab} and ρ_c along the two directions a and c:

$$\rho_{ab} = A_{ab}/T + B_{ab}T, \quad (3a)$$

$$\rho_c = A_c/T + B_cT. \quad (3b)$$

To compare our data with Eqs. (3a) and (3b), it is convenient to plot the product $\rho_c T$ against T^2 in order to test for a straight-line fit. We find that in all seven samples, Eqs. (3) provide a surprisingly good fit to both ρ_{ab} and ρ_c . The fit parameters are displayed in the table. Figure 4 shows the data for the out-of-plane resistivity plotted as $\rho_c T$ vs T^2 in five samples. With the exception of sample C, the fits are comparable in quality to those for ρ_{ab} . In sample C, however, a slight upwards curvature is discernible in the data. In view of the good fit of our data for both ρ_{ab} and ρ_c to Eqs. (3) and the reasonableness of the fit pa-

rameters obtained, we interpret our measurements as consistent with this novel mechanism, although the available range of ρ_c is limited. We plan to extend this test in crystals in which T_c is suppressed by selective doping through chemical substitution.

In conclusion, we have grown by a flux technique good quality crystals of $\text{YBa}_2\text{Cu}_3\text{O}_7$ and confirmed in seven samples that the out-of-plane ρ_c vs T is anomalous in the normal state, both in its temperature dependence and magnitude ($\sim 10 \text{ m}\Omega \text{ cm}$). The anisotropy (56–110 at 290 K increasing to 120–250 at T_c) indicates that the normal-state electronic structure is much more two-dimensional than previously appreciated. While the out-of-plane conductivity is close to the Mott limit, the in-plane conductivity implies large estimates for the metallic parameter k_{Fl} (31 at 100 K) and electronic mean free path (67 Å).

We have benefited from discussions with E. Abrahams, P. W. Anderson, G. Baskaran, and Z. Zou, and the assistance of Elaine Lenk in the SEMEDS measurements. This research is supported by the Department of Physics, Princeton University. S.J.H. was supported by the Garden-State Graduate Program.

¹J. G. Bednorz and K. A. Müller, *Z. Phys. B* **64**, 189 (1986).

²M. K. Wu, J. R. Ashburn, C. J. Torng, P. H. Hor, R. L. Meng, L. Gao, Z. J. Huang, Y. Q. Wang, and C. W. Chu, *Phys. Rev. Lett.* **58**, 908 (1987).

³T. R. Dingle, T. K. Worthington, W. J. Gallagher, and R. L. Sandstrom, *Phys. Rev. Lett.* **58**, 2687 (1987); T. K. Worthington, W. J. Gallagher, and T. R. Dinger, *ibid.* **59**, 1160 (1987); Y. Iye, T. Tamegai, H. Takeya, and H. Takei, *Jpn. J. Appl. Phys.* **26**, L1057 (1987).

⁴S. W. Tozer, A. W. Kleinsasser, T. Penney, D. Kaiser, and F. Holtzberg, *Phys. Rev. Lett.* **59**, 1768 (1987).

⁵Z. Z. Wang, J. Horvath, and N. P. Ong (unpublished).

⁶N. P. Ong, Z. Z. Wang, and J. McFarlane (unpublished).

⁷M. Hervieu, B. Domenges, C. Michel, and B. Raveau, *Europhys. Lett.* **4**, 205 (1987); E. A. Hewat, M. Dupuy, A. Bourret, J. J. Capponi, and M. Marezio, *Solid State Commun.* **64**, 517 (1987).

⁸Gordon Thomas (private communication).

⁹H. C. Montgomery, *J. Appl. Phys.* **42**, 2971 (1971).

¹⁰B. F. Logan, S. O. Rice, and R. F. Wick, *J. Appl. Phys.* **42**, 2975 (1971).

¹¹See, for e.g., Claire Schlenker, in *Low-Dimensional Conductors and Superconductors*, edited by D. Jerome and L. G. Caron, NATO Advanced Study Institute, Series B Physics, Vol. 155 (Plenum, New York, 1987).

¹²See, for e.g., Keizo Murata, Takashi Ukachi, Hiroyuki Anzai, Gunzi Saito, Koji Kajimura, and Takehiko Ishiguro, *J. Phys. Soc. Jpn.* **51**, 1817 (1982).

¹³P. B. Allen, W. E. Pickett, and H. Krakauer, *Phys. Rev. B* **36**, 3926 (1987).

¹⁴P. W. Anderson and Z. Zou, *Phys. Rev. Lett.* **60**, 132 (1988).

¹⁵P. W. Anderson, *Science* **235**, 1196 (1987); P. W. Anderson, G. Baskaran, Z. Zou, and T. Hsu, *Phys. Rev. Lett.* **58**, 2790 (1987).

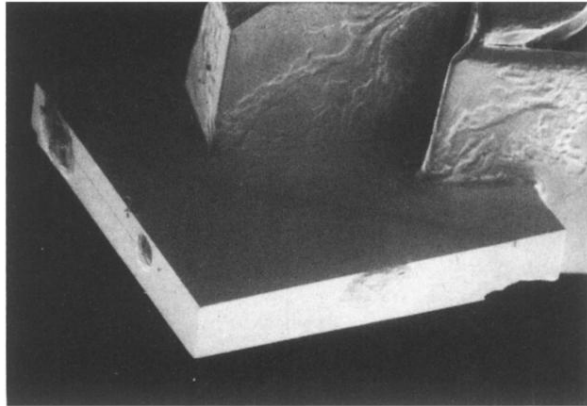


FIG. 1. Scanning electron micrograph of a typical crystal grown by the flux method. The as-grown crystals are superconducting above 90 K and orthorhombic with $\theta \sim 2^\circ$ (see text).